Research article JHEP|Reports

Saturated fatty acid-enriched small extracellular vesicles mediate a crosstalk inducing liver inflammation and hepatocyte insulin resistance

Authors

Irma Garcia-Martinez, **Rosa Alen**, Laura Pereira, Adrián Povo-Retana, Alma M. Astudillo, Ana B. Hitos, Isabel Gomez-Hurtado, Eduardo Lopez-Collazo, Lisardo Boscá, Rubén Francés, Ignacio Lizasoain, María Ángeles Moro, Jesús Balsinde, Manuel Izquierdo, Ángela M. Valverde

Correspondence

irmagarcia@iib.uam.es (I. Garcia-Martinez), avalverde@iib.uam.es (Á.M. Valverde).

Graphical abstract

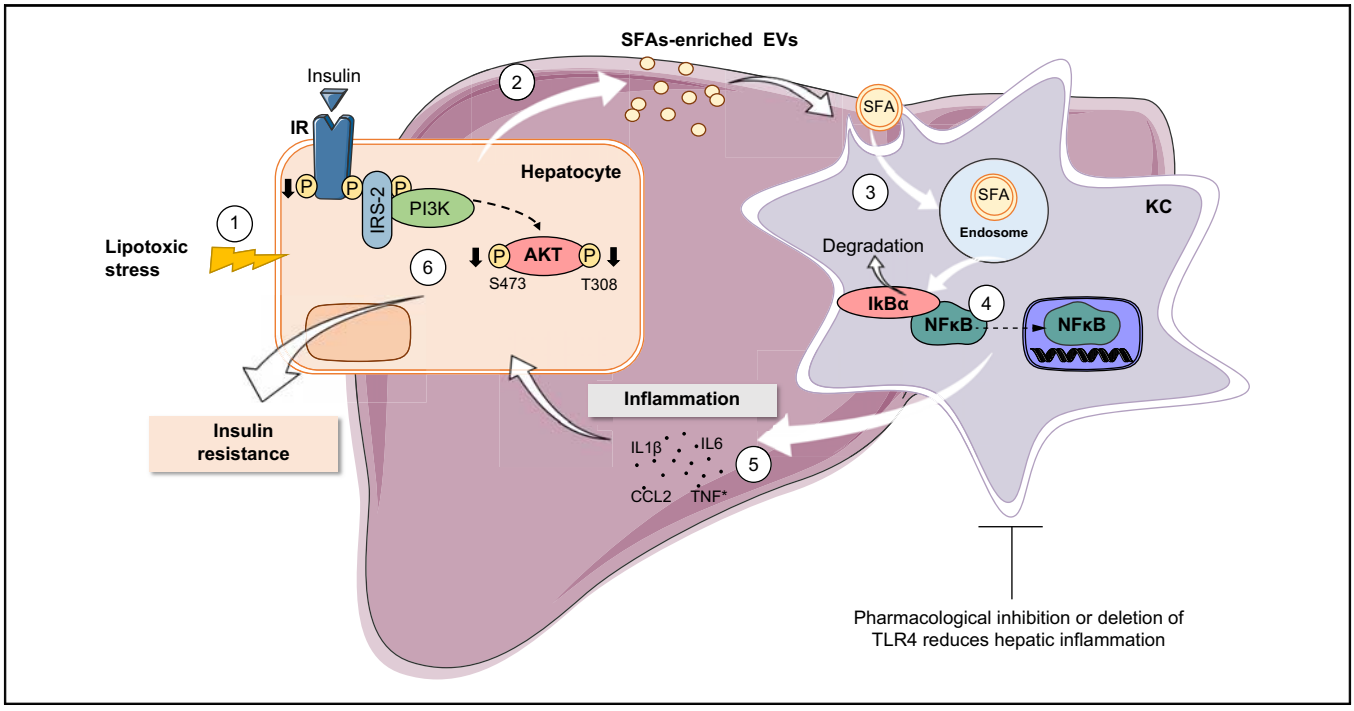

Highlights

- SFA-enriched sEV induce macrophage/Kupffer cells inflammation via TLR4.
- Lipotoxic sEV impair hepatocyte insulin signalling via macrophages/Kupffer cells.
- Lipotoxic sEV target Kupffer cells and induce liver inflammation *in vivo*.
- Pharmacological inhibition or deletion of TLR4 ameliorates liver inflammation induced by lipotoxic sEV.
- Lipotoxic sEV-mediated macrophage–hepatocyte crosstalk was found in patients with NAFLD.

Impact and Implications

Small extracellular vesicles (sEV) released by the hepatocytes under non-alcoholic fatty liver disease (NAFLD) conditions cause liver inflammation and insulin resistance in hepatocytes via paracrine hepatocyte–macrophage–hepatocyte crosstalk. We identified sEV as transporters of saturated fatty acids (SFAs) and potent lipotoxic inducers of liver inflammation. TLR4 deficiency or its pharmacological inhibition ameliorated liver inflammation induced by hepatocyte-derived lipotoxic sEV. Evidence of this macrophage–hepatocyte interactome was also found in patients with NAFLD, pointing to the relevance of sEV in SFA-mediated lipotoxicity in NAFLD.

https://doi.org/10.1016/j.jhepr.2023.100756

Research article

JHEP|Reports

Saturated fatty acid-enriched small extracellular vesicles mediate a crosstalk inducing liver inflammation and hepatocyte insulin resistance

Irma Garcia-Martinez,[1,2,†,*] **Rosa Alen**,[1,2,†] Laura Pereira,[2,3] Adrián Povo-Retana,[1] Alma M. Astudillo,[2,3] Ana B. Hitos,[1,2] Isabel Gomez-Hurtado,[4,5] Eduardo Lopez-Collazo,[6] Lisardo Boscá,[1,6,7] Rubén Francés,[4,5,8] Ignacio Lizasoain,[9,10] María Ángeles Moro,[11] Jesús Balsinde,[2,3] Manuel Izquierdo,[1] Ángela M. Valverde[1,2,*]

[1]Instituto de Investigaciones Biomédicas (IIBm) Alberto Sols (CSIC-UAM), Madrid, Spain; [2]Centro de Investigación Biomédica en Red de Diabetes y Enfermedades Metabólicas asociadas (CIBERdem), Instituto de Salud Carlos III, Madrid, Spain; [3]Instituto de Biología y Genética Molecular, Consejo Superior de Investigaciones Científicas (CSIC), Valladolid, Spain; [4]Instituto de Investigación Sanitaria ISABIAL, Hospital General Universitario Alicante, Alicante, Spain; [5]Centro de Investigación Biomédica en Red en Enfermedades Hepáticas y Digestivas (CIBERehd), Instituto de Salud Carlos III, Madrid, Spain; [6]Instituto de Investigación Sanitaria La Paz (IdiPaz), Hospital Universitario La Paz, Madrid, Spain; [7]Centro de Investigación Biomédica en Red en Enfermedades Cardiovasculares (CIBERcv), Instituto de Salud Carlos III, Madrid, Spain; [8]Dpto. Medicina Clínica, Universidad Miguel Hernández, San Juan de Alicante, Spain; [9]Unidad de Investigación Neurovascular, Departamento de Farmacología y Toxicología, Facultad de Medicina, Universidad Complutense, Madrid, Spain; [10]Instituto de Investigación Hospital 12 de Octubre (i+12), Madrid, Spain; [11]Neurovascular Pathophysiology Group, Centro Nacional de Investigaciones Cardiovasculares Carlos III (CNIC), Madrid, Spain

JHEP Reports **2023.** https://doi.org/10.1016/j.jhepr.2023.100756

Background & Aims: Lipotoxicity triggers non-alcoholic fatty liver disease (NAFLD) progression owing to the accumulation of toxic lipids in hepatocytes including saturated fatty acids (SFAs), which activate pro-inflammatory pathways. We investigated the impact of hepatocyte- or circulating-derived small extracellular vesicles (sEV) secreted under NAFLD conditions on liver inflammation and hepatocyte insulin signalling.

Methods: sEV released by primary mouse hepatocytes, characterised and analysed by lipidomics, were added to mouse macrophages/Kupffer cells (KC) to monitor internalisation and inflammatory responses. Insulin signalling was analysed in hepatocytes exposed to conditioned media from sEV-loaded macrophages/KC. Mice were i.v. injected sEV to study liver inflammation and insulin signalling. Circulating sEV from mice and humans with NAFLD were used to evaluate macrophage–hepatocyte crosstalk.

Results: Numbers of sEV released by hepatocytes increased under NAFLD conditions. Lipotoxic sEV were internalised by macrophages through the endosomal pathway and induced pro-inflammatory responses that were ameliorated by pharmacological inhibition or deletion of Toll-like receptor-4 (TLR4). Hepatocyte insulin signalling was impaired upon treatment with conditioned media from macrophages/KC loaded with lipotoxic sEV. Both hepatocyte-released lipotoxic sEV and the recipient macrophages/KC were enriched in palmitic (C16:0) and stearic (C18:0) SFAs, well-known TLR4 activators. Upon injection, lipotoxic sEV rapidly reached KC, triggering a pro-inflammatory response in the liver monitored by Jun N-terminal kinase (JNK) phosphorylation, NF-κB nuclear translocation, pro-inflammatory cytokine expression, and infiltration of immune cells into the liver parenchyma. sEV-mediated liver inflammation was attenuated by pharmacological inhibition or deletion of TLR4 in myeloid cells. Macrophage inflammation and subsequent hepatocyte insulin resistance were also induced by circulating sEV from mice and humans with NAFLD.

Conclusions: We identified hepatocyte-derived sEV as SFA transporters targeting macrophages/KC and activating a TLR4-mediated pro-inflammatory response enough to induce hepatocyte insulin resistance.

Impact and Implications: Small extracellular vesicles (sEV) released by the hepatocytes under non-alcoholic fatty liver disease (NAFLD) conditions cause liver inflammation and insulin resistance in hepatocytes via paracrine hepatocyte–macrophage–hepatocyte crosstalk. We identified sEV as transporters of saturated fatty acids (SFAs) and potent lipotoxic inducers of liver inflammation. TLR4 deficiency or its pharmacological inhibition ameliorated liver inflammation induced by hepatocyte-derived lipotoxic sEV. Evidence of this macrophage–hepatocyte interactome was also found in patients with NAFLD, pointing to the relevance of sEV in SFA-mediated lipotoxicity in NAFLD.

Keywords: NAFLD; Lipotoxicity; Inflammation; Insulin resistance; Extracellular vesicles; TLR4.
Received 7 July 2022; received in revised form 24 March 2023; accepted 28 March 2023; available online 7 April 2023
† These authors contributed equally to this work.
* Corresponding authors. Address: C/ Arturo Duperier 4, 28029, Madrid, Spain. Tel.: +34-91-9654498.
E-mail addresses: irmagarcia@iib.uam.es (I. Garcia-Martinez), avalverde@iib.uam.es (Á.M. Valverde).

Introduction

Non-alcoholic fatty liver disease (NAFLD) affects 25% of the adult population, especially in Western countries.[1] NAFLD is associated with obesity, insulin resistance, type 2 diabetes, and cardiovascular complications, and is considered the hepatic manifestation of metabolic syndrome.[2] NAFLD extends from non-alcoholic fatty liver towards non-alcoholic steatohepatitis (NASH) with variable degrees of inflammation and fibrosis and, ultimately, hepatocarcinoma. NAFLD is recently renamed as metabolic dysfunction-associated fatty liver disease to better define the disease as a broader metabolic disorder regarding its origin, progression, and outcomes.[3]

The underlying triggers/mechanisms of NAFLD progression are complex and multifactorial. To date, the most widely accepted hypothesis is the 'multiple-hit model'.[4] In this condition, excessive free fatty acid uptake by hepatocytes may overwhelm their capacity to esterify them into triglycerides, leading to the accumulation of toxic species including saturated fatty acids (SFAs) (*i.e.* palmitic acid [PA; C16:0] and stearic acid [SA; C18:0]) free cholesterol, and ceramides.[5] This abnormal cellular lipid composition, so-called lipotoxicity, eventually leads to organelle dysfunction, chronic inflammation, and apoptosis of the hepatocytes, hallmarks strongly associated with NAFLD progression to NASH.[6]

Apart from lipotoxicity, SFAs trigger pro-inflammatory responses by binding to and activating damage-associated molecular pattern receptors including Toll-like receptor-4 (TLR4).[6,7] Although both parenchymal and non-parenchymal liver cells express TLR4, the higher TLR4 expression is contributed by Kupffer cells (KC).[8] Along with other immune cells, KC integrate the innate immune system, which, aside from lipotoxicity, also plays a critical role in NAFLD progression.[9] In addition, lipotoxic hepatocyte damage during NAFLD can activate other immune cell populations and liver cells such as liver sinusoidal endothelial cells and hepatic stellate cells, boosting inflammation and fibrosis. Therefore, NASH progression seems to be the result of a complex intrahepatic interactome.[10]

Extracellular vesicles (EV) are mediators of cell-to-cell communication in health and disease.[11] The generic term 'EV' comprises heterogeneous populations of cell-released, nanometer-sized vesicles enclosed by a lipid bilayer membrane that contain bioactive cargo molecules partially reflecting the parental cell lineage. Exosomes, the smallest EV (30–150 nm), originate from intracellular multivesicular bodies, whereas shedding microvesicles (50–1,000 nm) directly bud from the plasma membrane.[12] However, it is now recommended to use operational terms to refer to EV such as size ('small EV' [sEV; size <200 nm] and 'medium/large EVs' [size >200 nm]), density, or biochemical composition.[13] Following their release, EV interact with target cells, in which they may elicit multiple functional responses and phenotypic changes.

Several studies reported that abnormal EV released by different cells might directly or indirectly induce insulin resistance in type 2 diabetes associated with NAFLD.[14,15] In particular, upon toxic lipid overload, hepatocytes release EV expressing tumour necrosis factor-related apoptosis-inducing ligand (TRAIL), which activates macrophages towards a pro-inflammatory phenotype (M1) via NF-κB signalling.[16] Nonetheless, the specific role of EV in the hepatocyte–macrophage paracrine interactome related to inflammation-associated insulin resistance during NAFLD remains to be established. In this study, we analysed sEV released by primary hepatocytes (PH) and circulating sEV (Circ-sEV) under lipotoxic conditions of NAFLD and their impact on macrophage/KC inflammation and, ultimately, on hepatocyte insulin signalling.

Materials and methods

Animal care and use

Male mice on the C57BL/6J genetic background were maintained at the animal facilities of the IIBm Alberto Sols (CSIC-UAM, Madrid, Spain). C57BL/6J male mice with global ($TLR4^{-/-}$) or specific deletion of TLR4 in myeloid cells ($TLR4^{\Delta Mye}$) and their respective controls ($TLR4^{+/+}$ and $TLR4^{fl/fl}$) were also used. Animals included in the study were controlled following the recommendations of the Federation of European Laboratory Animal Science Associations on health monitoring. Animals were randomly assigned to experimental groups. Control mice were fed a standard chow diet (CHD; 8.4% kcal from fat, A04, Panlab, Barcelona, Spain). To induce obesity and NAFLD, mice were fed a high-fat diet (HFD; 60% of kcal from fat, TD-06414, Envigo RMS, Blackthorn, UK) for 14 weeks starting at week 8 after birth. To induce NASH without obesity, male mice were fed a methionine–choline-deficient (MCD) diet (TD-90262, Envigo RMS) for 8 weeks starting at 14–16 weeks of age. All experimental procedures were approved by the IIBm and CSIC Animal Care and Use Committees and authorised by the Comunidad de Madrid.

Statistical analysis

Statistical analysis was performed using GraphPad Prism 8 software (San Diego, CA, USA). Statistical details are provided in each figure legend. Differences between two groups were compared using the Mann–Whitney *U* test. The Pearson correlation test was used to establish correlations between analytical/clinical parameters and the number of sEV/inflammatory cytokines in human studies. Lipid quantitative data were analysed using two-way ANOVA, followed by the Bonferroni *post hoc* test. Data are expressed as the mean ± SEM. A p value of less than 0.05 was considered significant. Mice and cells were randomly and blindly distributed for the treatments by investigators. Investigators were not blind in outcome assessment.

For further details regarding the materials and methods used, please refer to the Supplementary information.

Results

Lipotoxic conditions increase the release of sEV by PH

We first characterised the sEV released by two sources of PH exposed to lipotoxic conditions: hepatocytes treated for 24 h with 800 μM PA, which is an SFA present in Western diets that mimics lipotoxicity *in vitro*, or hepatocytes from mice fed a HFD for 14 weeks. For sEV isolation, PH were seeded at equal cell densities. Oil Red O staining confirmed intracellular lipid accumulation in hepatocytes either treated with PA or isolated from obese mice (Fig. S1A and B). Furthermore, we ensured that PH preserved their cellular viability according to the Minimal

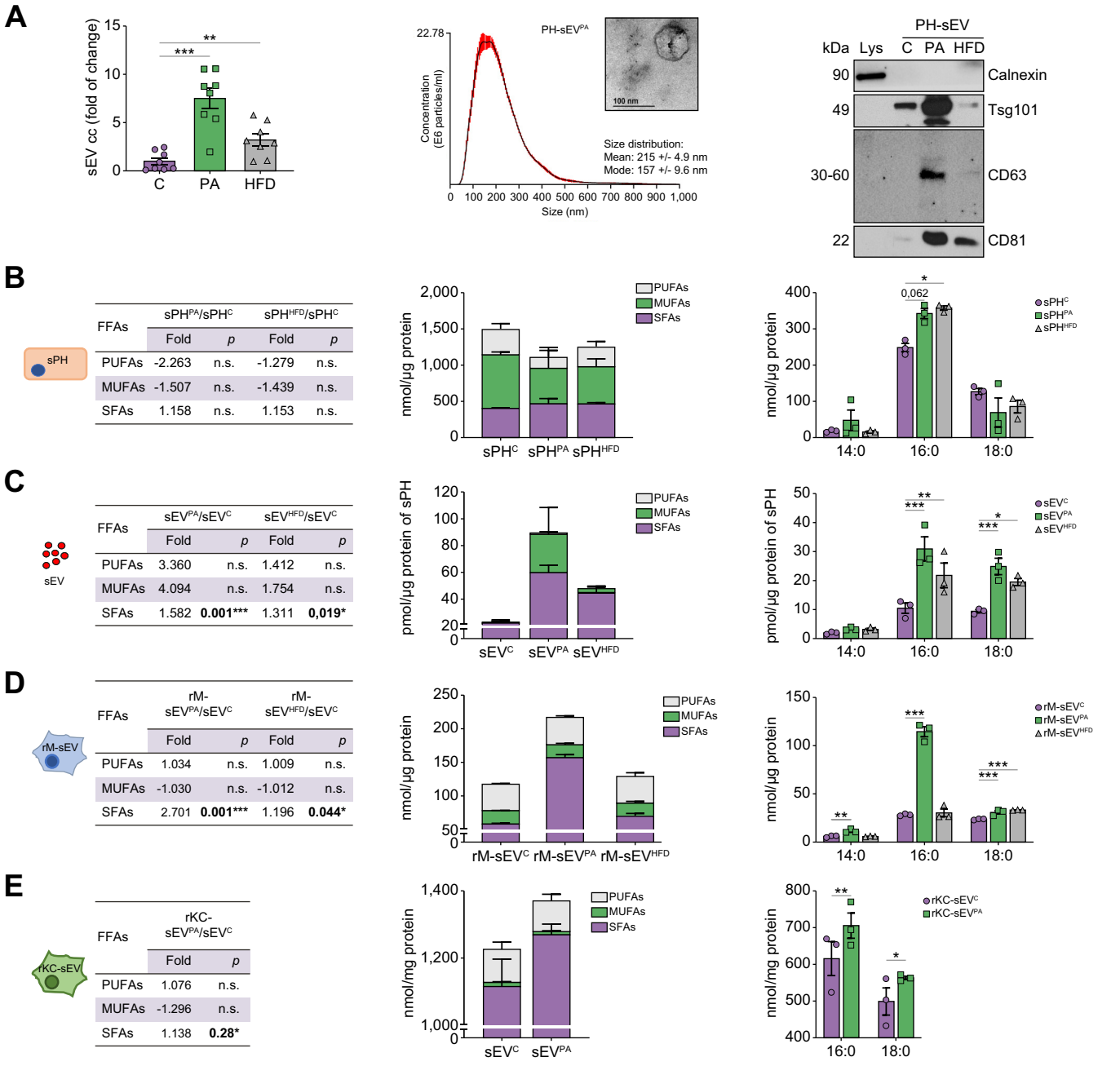

Fig. 1. Characterisation of the sEV released by PH under lipotoxic conditions and SFA content. (A) Quantification of sEV cc released to the culture medium by NTA (n = 8/group) (left panel). Representative NTA and TEM photomicrograph (scale bar, 100 nm) from sEV^{PA} (middle panel). Expression of sEV markers and Calnexin in sEV (right panel). Lysates from primary hepatocytes (Lys) were used as control. (B–E) Lipidomic analysis (n = 3/group). Total FFA content chart (left panel) and bar graph (middle panel) and SFA distribution (right panel) in PH secreting sEV (B), sEV (C), rM (D), and rKC (E). Data are expressed as the mean ± SEM. $^{**}p$ <0.01, $^{***}p$ <0.001, compared with sEV^{C}, Mann–Whitney U test (A). $^{*}p$ <0.05, $^{**}p$ <0.01, $^{***}p$ <0.001 compared with sPH^{C} (B), sEV^{C} (C), rM-sEV^{C} (D), or rKC-sEV^{C} (E), Two-way ANOVA, Bonferroni *post hoc* test. cc, concentration; FFA, free fatty acid; HFD, high-fat diet; MUFA, monounsaturated fatty acid; NTA, nanoparticle tracking analysis; PA, palmitic acid; PH, primary hepatocytes; PUFA, polyunsaturated fatty acid; rKC, recipient primary Kupffer cells; rM, recipient peritoneal macrophages; sEV, mall extracellular vesicles; SFA, saturated fatty acid; sPH, secreting PH; TEM, transmission electron microscopy.

Information for Studies of Extracellular Vesicles (MISEV) guidelines[13] and did not show apoptotic features such as caspase-3 cleavage or apoptotic nuclei (Fig. S2A–C).

sEV, purified from equal volumes of culture media and similar cell numbers, were quantified by nanoparticle tracking analysis (NTA) and characterised by transmission electron microscopy (TEM) and Western blot (Fig. 1A and Fig. S3) as recommended by MISEV. According to NTA, PH exposed to a lipotoxic environment (PA-treated or from HFD-fed mice) significantly released more sEV (referred to as sEV^{PA} or sEV^{HFD}, respectively) compared with PH isolated from CHD-fed mice (sEV^{C}). TEM confirmed that sEV size ranged within the diameter previously described for sEV

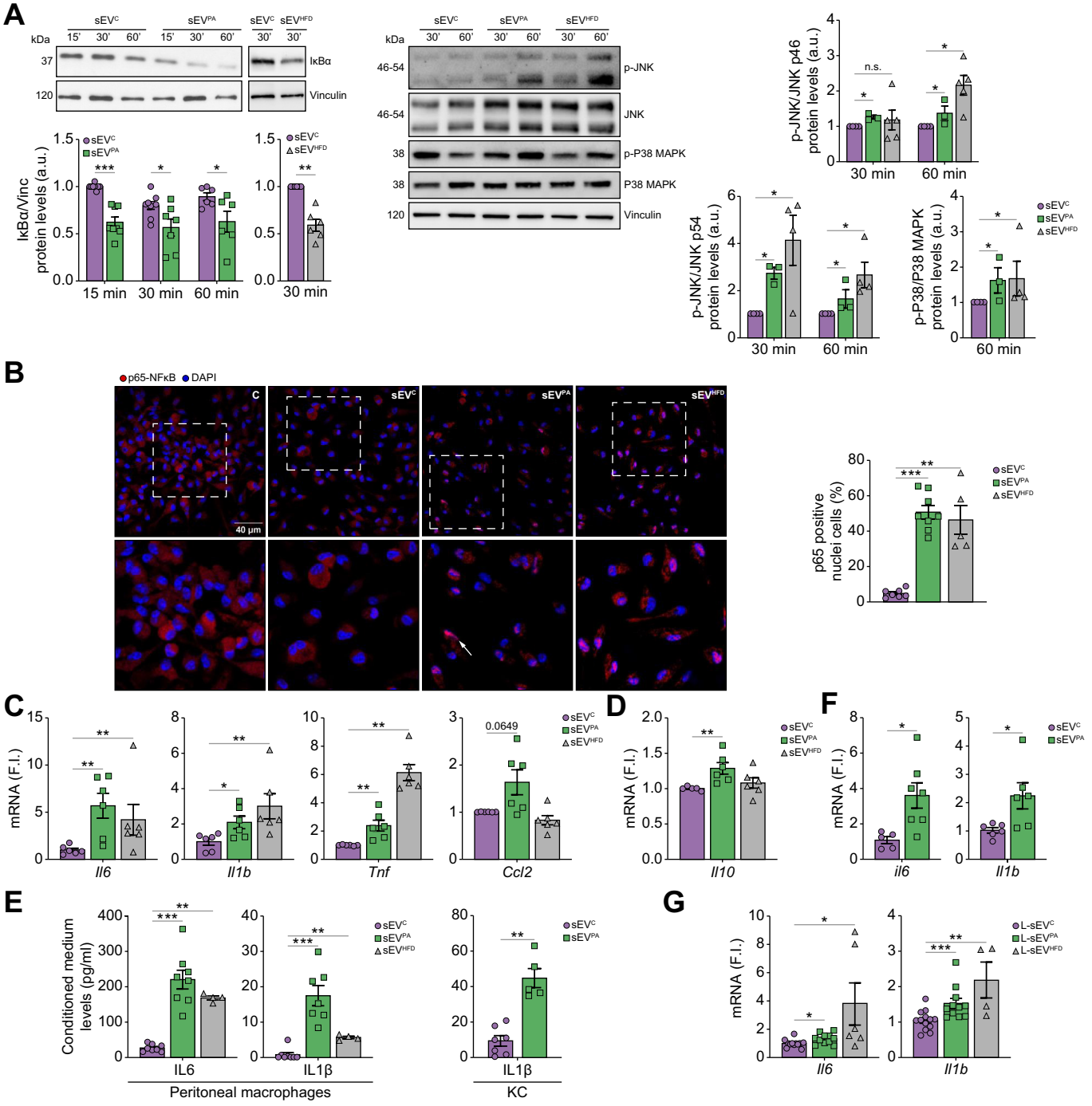

Fig. 2. sEV released by lipotoxic PH trigger inflammation in macrophages. (A) Western blot analysis with the indicated antibodies IκBα (n = 5–8/group), and pJNK/JNK and pP38 MAPK/P38 MAPK (n = 3–5/group), and quantification. (B) p65-NF-κB nuclear translocation by immunofluorescence (red) counterstaining with DAPI (blue) (left panel). Arrows point to p65-NF-κB-positive nuclei (scale bar, 40 μm) (right panel). Quantification of the percentage of cells with p65-NF-κB nuclear translocation (n = 5–8/group). (C) *Il-6*, *Il-1β*, *Tnf*, and *Ccl2* mRNA levels and (D) *Il-10* mRNA levels in peritoneal macrophages incubated with sEV for 8 h (n = 5–6/group). (E) IL-6 and IL-1β released to the culture supernatants by peritoneal macrophages (left panel) and IL-1β released to the culture supernatants by KC (right panel) receiving sEV for 8 h (n = 4–8/group). (F) *Il-6* and *Il-1β* mRNA levels in peritoneal macrophages treated with 10 μg of sEV^{C} or sEV^{PA} for 8 h (n = 5–7/group). (G) *Il-6* and *Il-1β* mRNA levels in peritoneal macrophages after incubation with the lipid fraction from sEV ($L\text{-}sEV^{C}$, $L\text{-}sEV^{PA}$, and $L\text{-}sEV^{HFD}$) for 8 h (n = 4–13/group). Data are expressed as the mean ± SEM. *p <0.05, **p <0.01, ***p <0.001, compared with sEV^{C}, Mann–Whitney *U* test. a.u., arbitrary units; FI, fold induction; HFD, high-fat diet; JNK, Jun N-terminal kinase; KC, Kupffer cells; MAPK, mitogen-activated protein kinase; PA, palmitic acid; PH, primary hepatocytes; sEV, small extracellular vesicles.

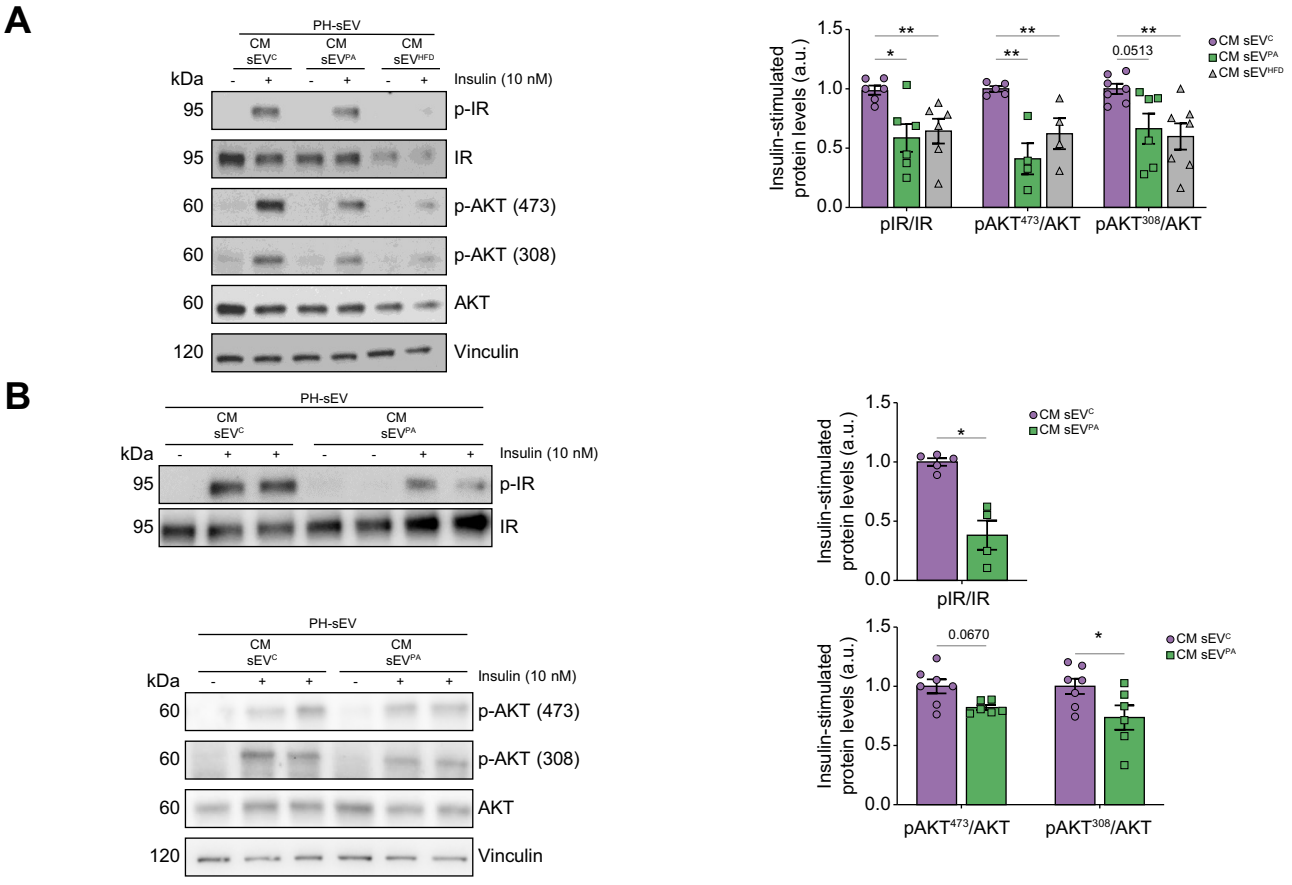

Fig. 3. CM from peritoneal macrophages and KC treated with lipotoxic sEV induces insulin resistance in PH. PH were incubated for 24 h with CM collected from peritoneal macrophages (A) or KC (B) previously treated with sEV for 24 or 8 h, respectively. Then hepatocytes were stimulated with insulin (10 nM) for a further 10 min. Phosphorylation of IR and AKT was analysed by Western blot and normalised by total IR and AKT levels. Representative Western blots and quantification are shown (n = 4–7/group). Data are expressed as the mean ± SEM. $^{*}p$ <0.05, $^{**}p$ <0.01, compared with CM sEV^{C}, Mann–Whitney *U* test. a.u., arbitrary units; CM, conditioned medium; IR, insulin receptor; KC, Kupffer cells; PA, palmitic acid; PH, primary hepatocytes; sEV, small extracellular vesicles.

and, likewise, all fractions expressed sEV-specific markers (Tsg101, CD63, and CD81), whereas calnexin, an endoplasmic reticulum marker, was absent in sEV.

Characterisation of the uptake of hepatocyte-released sEV by macrophages

We next evaluated the internalisation of PH-released sEV by macrophages. Peritoneal mouse macrophages were treated with sEV (sEV^{C}, sEV^{PA}, and sEV^{HFD}) labelled with the PKH67 probe, and fluorescent intracellular labelling was visualised after 2 min (Fig. S4A). Live cell imaging showed a progressive accumulation of the three types of labelled sEV into the macrophages (Movies S1–S3).

Supplementary data to this article can be found online at https://doi.org/10.1016/j.jhepr.2023.100756.

The following are the supplementary data to this article:- Supplementary Video S1. Supplementary Video S2. Supplementary Video S3.

Colocalisation of sEV with early endosome antigen 1 (EEA1), an early endosomal membrane-associated protein,[17] was found (Fig. S4B); this effect declined after 15 min (Fig. S5A). Notably, the colocalisation of sEV with the early endosome occurred independently of the hepatocyte source of the sEV. Moreover, colocalisation of sEV and Rab7, a small GTPase of the late endosomal compartment,[18] was observed at 40 min (Fig. S5B), pointing to rapid internalisation of hepatocyte-released sEV into the macrophages.

sEV released by hepatocytes under lipotoxic conditions transferred SFAs to the macrophages/KC

We next conducted a lipidomic analysis of PH secreting the sEV (sPH^{C}, sPH^{PA}, and sPH^{HFD}), sEV (sEV^{C}, sEV^{PA}, and sEV^{HFD}), and recipient peritoneal macrophages (rM-sEV) or primary KC (rKC-sEV) as schematised in Fig. S6. We found an increase in SFAs in sEV released by lipotoxic PH, an effect mainly owing to a significant rise in PA and SA (Fig. 1C, right panel; and Table S1). However, PA, but not SA, increased in lipotoxic PH (Fig. 1B, right panel). Likewise, the total content of monounsaturated fatty acids (MUFAs) increased in sEV^{PA} and sEV^{HFD} fractions (Fig. 1C, middle and left panels) in contrast to sPH^{PA} and sPH^{HFD}, where we found a decrease (Fig. 1B, middle and left panels), particularly in 18:1n-9 and 18:2n-6 species (Table S2).

We also analysed rM-sEV. As shown in Fig. 1D (middle and left panels), a substantial elevation in SFAs were detected in those treated with sEV^{PA} and sEV^{HFD}. In peritoneal macrophages loaded with sEV^{PA}, the increase was attributable to a gain in C14:0 (myristic acid), PA, and SA, whereas in peritoneal macrophages receiving sEV^{HFD}, the increment was found only in SA

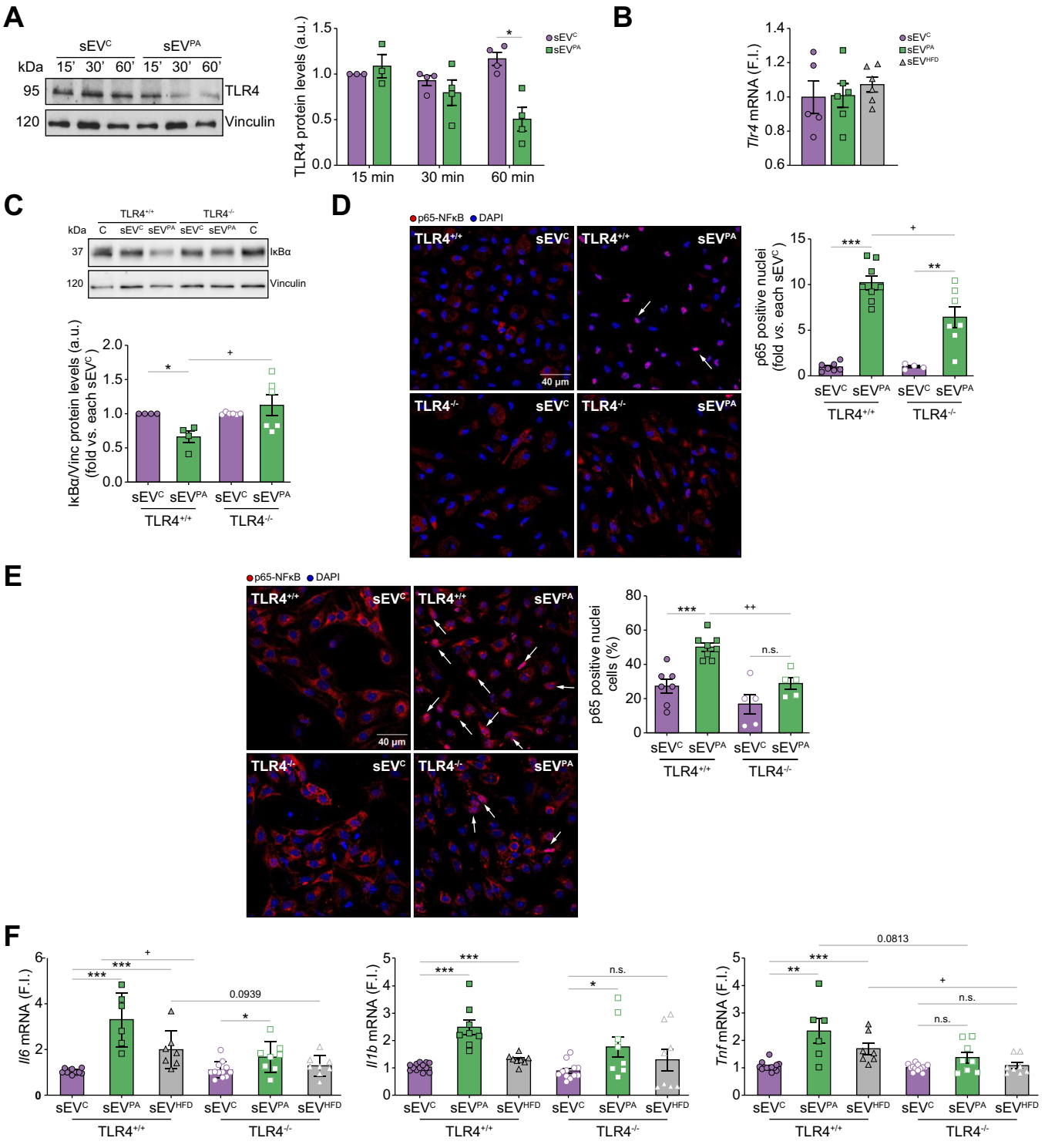

Fig. 4. TLR4/NF-κB signalling pathway plays a role in macrophage/KC inflammation induced by lipotoxic sEV released by PH. (A) Representative Western blots and quantification (n = 3–4/group). (B) *Tlr4* mRNA levels in peritoneal macrophages incubated with sEV for 8 h (n = 5–6/group). (C) Peritoneal macrophages from wild-type (TLR4$^{+/+}$) and TLR4$^{-/-}$ mice were incubated with sEV for 15 min. Representative blots and quantification (n = 4–6/group). Peritoneal macrophages (D) and KC (E) from TLR4$^{+/+}$ and TLR4$^{-/-}$ mice were incubated with sEV for 1 h. Representative images are shown (scale bar, 40 μm). Arrows point to p65-NF-κB-positive nuclei (left panel). Quantification of cells with p65-NFκB nuclear translocation (fold *vs.* each sEV^{C}) (right panel) (n = 4–8/group). (F) KC from TLR4$^{+/+}$ and TLR4$^{-/-}$ mice were incubated with sEV for 8 h. *Il-6*, *Il-1β*, and *Tnf* mRNA levels (n = 6–13/group). Data are expressed as the mean ± SEM. In (A), $^{*}p$ <0.05, compared with sEV^{C}. In (C)–(F), $^{*}p$ <0.05, $^{**}p$ <0.01, $^{***}p$ <0.001, compared with sEV^{C} from the same genotype, and ^{+}p <0.05, ^{++}p <0.01, compared with the same condition in TLR4$^{+/+}$ mice, Mann–Whitney *U* test. a.u., arbitrary units; FI, fold induction; HFD, high-fat diet; KC, Kupffer cells; PA, palmitic acid; PH, primary hepatocytes; sEV, small extracellular vesicles; TLR4, Toll-like receptor-4.

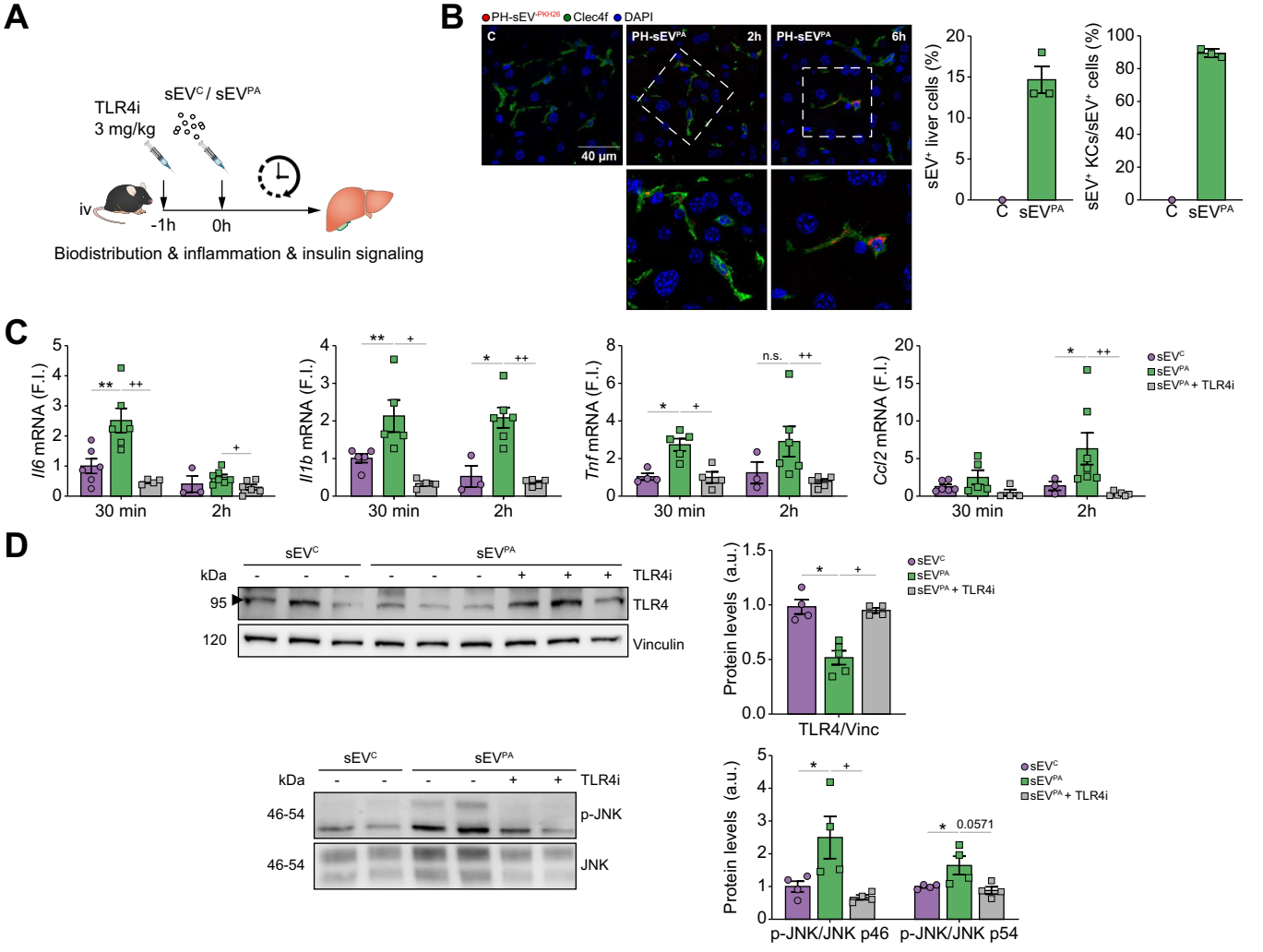

Fig. 5. ***In vivo*** **delivery of sEV released by lipotoxic PH targeted KC and induced a rapid inflammatory response in the liver.** (A) Experimental design of *in vivo* sEV injection. (B) PKH26-labelled sEV^{PA} (red) uptake by KC analysed by immunofluorescence using anti-Clec4f antibody (green) counterstaining with DAPI (blue). Representative liver images (scale bar, 40 μm) and percentage of sEV-positive liver cells and sEV-positive liver cells expressing Clec4f are shown (n = 3 sEV-injected mice). (C) Mice were i.v. injected or not TLR4 inhibitor (TLR4i) 1 h before sEV injection. *Il-6*, *Il-1β*, *Tnf*, and *Ccl2* mRNA levels in the liver are shown (n = 3–6/mice group). (D) TLR4 levels (n = 4–5 mice/group) and JNK phosphorylation (n = 4/mice group) in livers at 2 h post sEV injection analysed by Western blot and normalised with Vinculin and JNK, respectively. Representative blots and quantification are shown. Data are expressed as the mean ± SEM. In (C) and (D), $^{*}p$ <0.05, $^{**}p$ <0.01, compared with sEV^{C} and ^{+}p <0.05, ^{++}p <0.01 compared with sEV^{PA}, Mann–Whitney *U* test. a.u., arbitrary units; FI, fold induction; JNK, Jun N-terminal kinase; KC, Kupffer cells; PA, palmitic acid; PH, primary hepatocytes; sEV, small extracellular vesicles; TLR4, Toll-like receptor-4; TLR4i, TLR4 inhibitor.

(Fig. 1D, right panel; and Table S3). Transfer of SFAs by lipotoxic sEV^{PA} was verified in primary KC (Fig. 2E and Table S4). These results point sEV as new mediators of SFA transfer from hepatocytes to macrophages/KC, suggesting that sEV^{PA} and sEV^{HFD} may be intrinsically lipotoxic.

Lipotoxic sEV released by hepatocytes activate pro-inflammatory signalling in macrophages

NF-κB, a key transcription factor in innate immune pro-inflammatory signalling, is also involved in metabolic inflammation.[19] Likewise, phosphorylation of the pro-inflammatory mediators Jun N-terminal kinase (JNK) and p38 mitogen-activated protein kinase (MAPK) contributes to liver inflammation during NAFLD.[20] Degradation of the NF-κB inhibitor IκBα was found in peritoneal macrophages exposed to sEV^{PA} during 15–60 min (Fig. 2A) and p65-NF-κB nuclear translocation was visualised 1 h after the addition of the sEV^{PA} (Fig. 2B). Similar results were obtained in peritoneal macrophages loaded with sEV^{HFD} (Fig. 2A and B). In addition, phosphorylation of JNK and p38 MAPK was increased in macrophages treated with lipotoxic sEV (Fig. 2A).

We next characterised the inflammatory profile of peritoneal macrophages receiving lipotoxic sEV. Peritoneal macrophages were stimulated with sEV for 8 h, after which mRNA levels of pro- and anti-inflammatory cytokines were determined. Fig. 2C shows increased mRNA expression of *Il6*, *Il-1β*, and *Tnf* and the chemokine *Ccl2* in peritoneal macrophages receiving sEV^{PA} or sEV^{HFD} compared with those treated with sEV^{C}. We also found an increase in *Il-10* mRNA levels in macrophages receiving lipotoxic sEV^{PA}, suggesting an anti-inflammatory compensatory response.

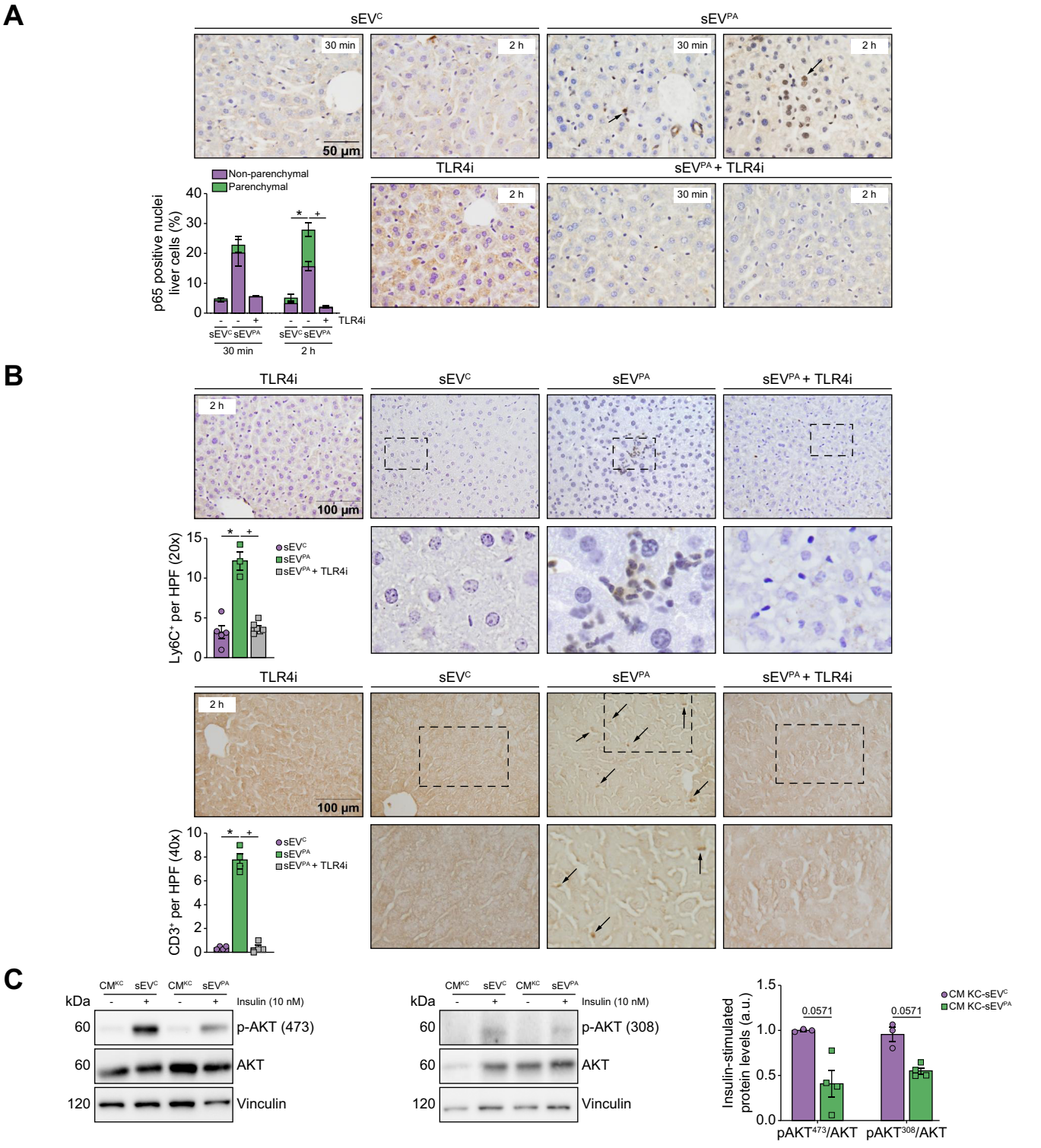

Fig. 6. The rapid inflammatory response induced by *in vivo* injection of PH-released lipotoxic sEV impairs insulin signalling in the liver. (A) Representative liver micrographs showing translocation of p65-NF-κB to the nucleus (scale bar, 50 μm) 30 min and 2 h after i.v. sEV injection. TLR4i was injected at 3 mg/kg to the corresponding group 1 h before sEV injection. Arrows point to p65-NF-κB-positive nuclei (scale bar, 50 μm). Percentage of liver cells (non-parenchymal and parenchymal) with p65-NF-κB nuclear translocation at 30 min and 2 h (n = 3–5 mice/group) are shown (lower left panel). (B) Representative micrographs of liver sections 2 h after sEV injection with the indicated antibodies. (upper panel) Ly6C-positive cells (scale bar, 100 μm) and quantification (n = 3–6 mice/group). (lower panel) CD3-positive cells (scale bar, 100 μm) and quantification (n = 3–4 mice/group). (C) KC, isolated from mice at 16 h post injection of sEV, were cultured for 16 h, and CM were collected. PH were incubated for 24 h with the CM collected from KC and then stimulated with insulin (10 nM) for 10 min. Representative Western blots of AKT phosphorylation normalised by AKT levels and quantifications (n = 3–4/mice group). Data are expressed as the mean ± SEM. In (A) and (B), $^{*}p$ <0.05 compared with sEV^{C}, ^{+}p <0.05 compared with sEV^{PA}, Mann–Whitney *U* test. a.u., arbitrary units; CM, conditioned medium; HPF, high-power field; KC, Kupffer cells; PA, palmitic acid; PH, primary hepatocytes; sEV, small extracellular vesicles; TLR4, Toll-like receptor-4; TLR4i, TLR4 inhibitor.

Of note, *Il-4* mRNA expression was not detected (results not shown). Moreover, peritoneal macrophages released IL-6 and IL-1β to the culture medium upon the addition of lipotoxic sEV, an effect validated in KC by determining IL-1β levels (Fig. 2E). A similar inflammatory response was observed when the amount of sEV added to peritoneal macrophages was normalised to their total protein content, as shown by comparable increases in *Il-6* and *Il-1β* mRNA levels (Fig. 2F). Furthermore, to relate sEV lipotoxicity to their pro-inflammatory effect, the lipid fraction of PH-derived sEV^{C}, sEV^{PA}, and sEV^{HFD} (L-sEV^{C}, L-sEV^{PA}, and L-sEV^{HFD}, respectively) was extracted and directly added to peritoneal macrophages. We found that *Il-6* and *Il-1β* mRNAs were also elevated when peritoneal macrophages were incubated with the lipid fraction of lipotoxic sEV (Fig. 2G).

CM from macrophages/KC treated with hepatocyte-derived lipotoxic sEV attenuated insulin signalling in hepatocytes

Considering the negative effect of the secretome released by PA-stimulated macrophages/KC in hepatocyte insulin signalling previously reported by our group,[21] we analysed insulin signalling in hepatocytes exposed to the CM released by macrophages loaded with sEV. Peritoneal macrophages were treated for 24 h with sEV^{C}, sEV^{PA}, or sEV^{HFD}. Then, the CM (CM sEV^{C}, CM sEV^{PA}, and CM sEV^{HFD}) were collected and added to hepatocytes for a further 24 h, after which insulin signalling was analysed. Fig. 3A shows decreased insulin receptor (IR) and AKT (Ser473/Thr308) phosphorylation in hepatocytes treated with CM sEV^{PA} or CM sEV^{HFD} compared with hepatocytes receiving CM sEV^{C}. Notably, CM sEV^{HFD} was more potent in reducing AKT Thr308 phosphorylation, suggesting an effect of additional components of this CM in boosting hepatocyte insulin resistance. Of note, IR and AKT phosphorylation was similar in hepatocytes incubated with CM sEV^{C} or CM collected from macrophages that did not receive sEV (Fig. S7). Again, similar results were obtained using the CM released by KC stimulated with lipotoxic sEV (Fig. 3B).

The relevance of the hepatocyte–macrophage–hepatocyte interactome mediated by the lipotoxic sEV was also evidenced by the mild effect of the direct treatment of hepatocytes with lipotoxic sEV before insulin stimulation (Fig. S8A) despite the marked accumulation of sEV into these cells at 2 h (Fig. S8B).

TLR4-dependent pro-inflammatory responses in macrophages loaded with lipotoxic hepatocyte-derived sEV

TLR4 binds SFAs,[22] thereby activating inflammatory signalling cascades. In unstimulated cells, TLR4 is present at the plasma membrane, and upon its activation, it is internalised, translocated to early endosomes, and then sorted for degradation in late endosomes and lysosomes.[23] In this regard, decreased TLR4 protein expression was found in peritoneal macrophages exposed to sEV^{PA} (Fig. 4A), suggesting a previous activation. By contrast, no changes in *Tlr4* mRNA expression were observed (Fig. 4B). To demonstrate activation of TLR4-dependent NF-κB signalling in macrophages exposed to lipotoxic sEV released by PH, peritoneal macrophages and KC from mice with global TLR4 deletion ($TLR4^{-/-}$) were used. As shown in Fig. 4C, sEV^{PA}-mediated degradation of IκBα was not detected in $TLR4^{-/-}$ peritoneal macrophages and, consistently, p65-NF-κB nuclear translocation was significantly decreased (Fig. 4D). In addition, pharmacological inhibition of TLR4 in peritoneal macrophages abolished IκBα degradation and counteracted p65-NF-κB nuclear translocation induced by lipotoxic sEV (Fig. S9A–E). Interestingly, p65-NF-κB nuclear translocation and the elevations in *Il-1β*, *Il-6*, and *Tnf* mRNAs induced by sEV^{PA} or sEV^{HFD} were attenuated in KC from $TLR4^{-/-}$ mice (Fig. 4E and F).

As sEV^{PA} or sEV^{HFD} are enriched in SFAs mainly PA and SA (Fig. 1C), peritoneal macrophages were directly stimulated with either PA (750 μM) or SA (350 μM). At 30 min, PA and SA increased JNK and p38 MAPK phosphorylation and triggered IκBα degradation. By contrast, these responses were markedly attenuated in $TLR4^{-/-}$ peritoneal macrophages (Fig. S10A and B). These results are consistent with previous findings showing TLR4-dependent effects of SFA-induced inflammation.[24]

Lipotoxic hepatocyte-derived sEV target KC, trigger pro-inflammatory signalling, and induce hepatic inflammation *in vivo*

We investigated the *in vivo* significance of our findings in liver inflammation during NAFLD. C57BL/6J mice were i.v. injected 50 μg of sEV (sEV^{C} or sEV^{PA}) (Fig. 5A). We previously checked that protein concentrations in sEV^{C} and sEV^{PA} measured by BCA assay contain equivalent numbers of particles analysed by NTA (sEV^{C} $6.56 \times 10^{8} \pm 2.46$ *vs.* sEV^{PA} $6.30 \times 10^{8} \pm 1.53$ in 5 μg of sEV protein, n = 4/group). The delivery of PKH26-labelled sEV to the liver was visualised at 2 and 6 h post injection (Fig. 5B), and, importantly, PKH26 immunofluorescence was located in Clec4f-positive cells, evidencing sEV internalisation by KC rather than by hepatocytes at this early time period. We evaluated inflammatory markers in the liver upon injection of sEV^{PA} or sEV^{C} and found a rapid increase in *Il-6*, *Il-1β*, and *Tnf* mRNAs as early as 30 min followed by *Ccl2* at 2 h post injection (Fig. 5C). At the molecular level, sEV^{PA} decreased TLR4 protein levels and increased JNK phosphorylation (Fig. 5D). Increased phospho-JNK was also found in mice i.v. injected sEV^{HFD} (Fig. S11A).

Liver inflammation was also visualised by nuclear p65-NF-κB immunohistochemistry. Fig. 6A shows areas of nuclear staining in non-parenchymal immune cells at 30 min post sEV^{PA} injection, whereas nuclear p65-NF-κB was visualised in hepatocytes at 2 h, suggesting an earlier effect of lipotoxic sEV in immune cells. The presence of foci of $Ly6C^{+}$ monocytes, as well as $CD3^{+}$ lymphocytes, in liver parenchyma at 2 h post sEV^{PA} injection (Fig. 6B) points to new recruitment of immune cells consistent with the increase in *Ccl2* expression. Again, similar effects were found in the livers of mice injected sEV^{HFD} (Fig. S11B and C).

In line with data depicted in Fig. S9, injection of the TLR4 inhibitor 1 h before sEV^{PA} administration prevented elevations in hepatic *Il-6*, *Il-1β*, *Tnf*, and *Ccl2* mRNAs; JNK phosphorylation; and the drop of TRL4 (Fig. 5C and D). Likewise, both nuclear p65-NF-κB translocation and infiltration of $Ly6C^{+}$ and $CD3^{+}$ cells were abolished in mice injected TLR4 inhibitor before sEV^{PA} (Fig. 5A and B). Of note, no effect was found upon injection of the TLR4 inhibition alone (Fig. 5A and B).

In vivo injection of lipotoxic hepatocyte-derived sEV targeting KC attenuates insulin-mediated signalling in hepatocytes

We next investigated whether KC mediate insulin resistance in hepatocytes upon *in vivo* injection of lipotoxic PH-sEV. Mice were injected sEV^{PA} or sEV^{C}, and after 16 h, KCs were isolated and cultured for 24 h. The CM (CM-sEV^{PA} or CM-sEV^{C}) was collected and used to treat PH for 24 h, after which insulin signalling was analysed. As shown in Fig. 6C, AKT phosphorylation (Ser473/Thr308), used as readout, was decreased in hepatocytes exposed to CM-sEV^{PA}, suggesting that lipotoxic sEV induce hepatocyte insulin resistance at least in part through activation of hepatic resident macrophages.

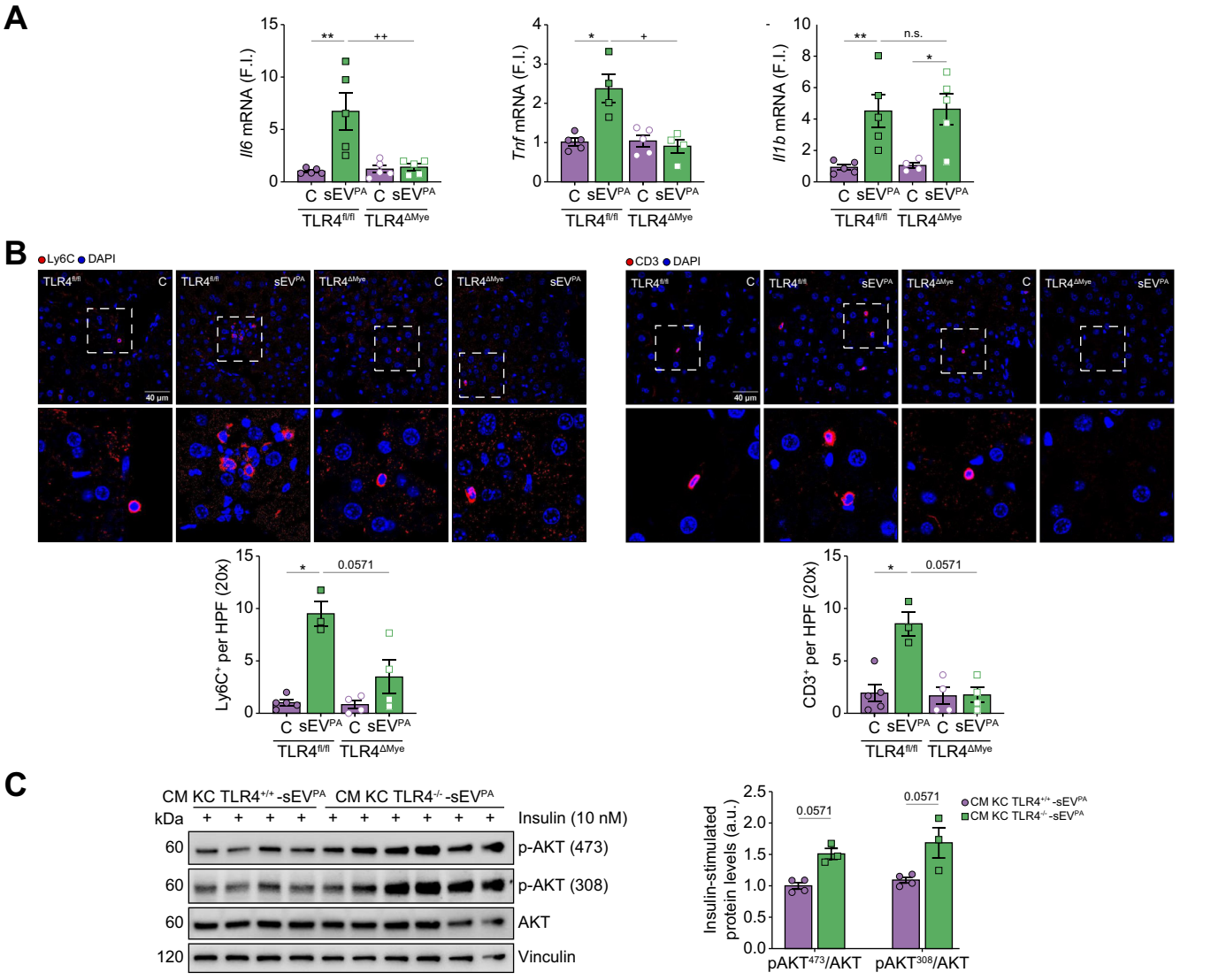

Fig. 7. sEV-mediated liver inflammation was reduced in mice with TLR4 deletion in myeloid cells. TLR4$^{fl/fl}$ and TLR4$^{\Delta Mye}$ mice were injected i.v. sEV^{PA} or PBS as control and sacrificed at 30 min or 2 h. (A) *Il-6*, *Il-1β*, and *Tnf* mRNA levels in the liver at 30 min post injection (n = 4–5/group). (B) Representative immunofluorescence images of liver sections 2 h after sEV injection with the indicated antibodies (n = 3–5/mice group). (upper panel) Ly6C-positive cells (scale bar, 40 μm) and quantification. (lower panel) CD3-positive cells (scale bar, 40 μm) and quantification. (C) KC, isolated from TLR4$^{+/+}$ and TLR4$^{-/-}$ mice at 16 h post injection of sEV^{PA}, were cultured for 16 h, and CM were collected and used to treat PH for 24 h prior to insulin stimulation (10 nM, 10 min). Representative Western blots of AKT phosphorylation normalised by AKT levels and quantifications (n = 3–4/mice group). Data are expressed as the mean ± SEM. In (A) and (B), $^{*}p$ <0.05, $^{**}p$ <0.01, compared with control from the same genotype, and ^{+}p <0.05, ^{++}p <0.01, compared with sEV^{PA} in TLR4$^{fl/fl}$ mice, Mann–Whitney *U* test. In (C) Mann–Whitney *U* test compared with sEV^{PA} in TLR4$^{+/+}$ mice. a.u., arbitrary units; CM, conditioned medium; FI, fold induction; HPF, high-power field; KC, Kupffer cells; PA, palmitic acid; PH, primary hepatocytes; sEV, small extracellular vesicles; TLR4, Toll-like receptor-4.

sEV-mediated liver inflammation was attenuated in mice with TLR4 deletion in myeloid cells

To confirm TLR4-dependent pro-inflammatory responses specifically in immune cells upon injection of lipotoxic sEV, mice with specific deletion of TLR4 in myeloid cells (TLR4$^{\Delta Mye}$) and their respective controls (TLR4$^{fl/fl}$) were used. As shown in Fig. 7A, TLR4$^{fl/fl}$ mice presented a rise in *Il-6*, *Il-1β*, and *Tnf* mRNA levels in the liver at 30 min post sEV^{PA} injection, whereas *Ccl2* mRNA was elevated at 2 h post injection. This effect was significantly attenuated in TLR4$^{\Delta Mye}$ mice regarding *Il-6*, *Tnf*, and *Ccl2* mRNAs. Moreover, at 2 h post sEV^{PA} injection, features of inflammation manifested by the presence of foci of Ly6C^{+}, as well as CD3^{+} cells into liver parenchyma, were observed in TLR4$^{fl/fl}$ mice, but not in TLR4$^{\Delta Mye}$ mice (Fig. 7B). Furthermore, insulin-induced AKT phosphorylation (Ser473/Thr308) in hepatocytes exposed to the CM released by KC from TLR4$^{-/-}$ mice was higher than AKT phosphorylation levels in hepatocytes treated with the CM released by KC from TLR4$^{+/+}$ mice (Fig. 7C).

Circ-sEV from mice and humans with NAFLD trigger inflammatory responses in macrophages and attenuate insulin signalling in hepatocytes

Because during NAFLD lipotoxic sEV have been detected in circulation,[25] we analysed the impact of Circ-sEV from mice and

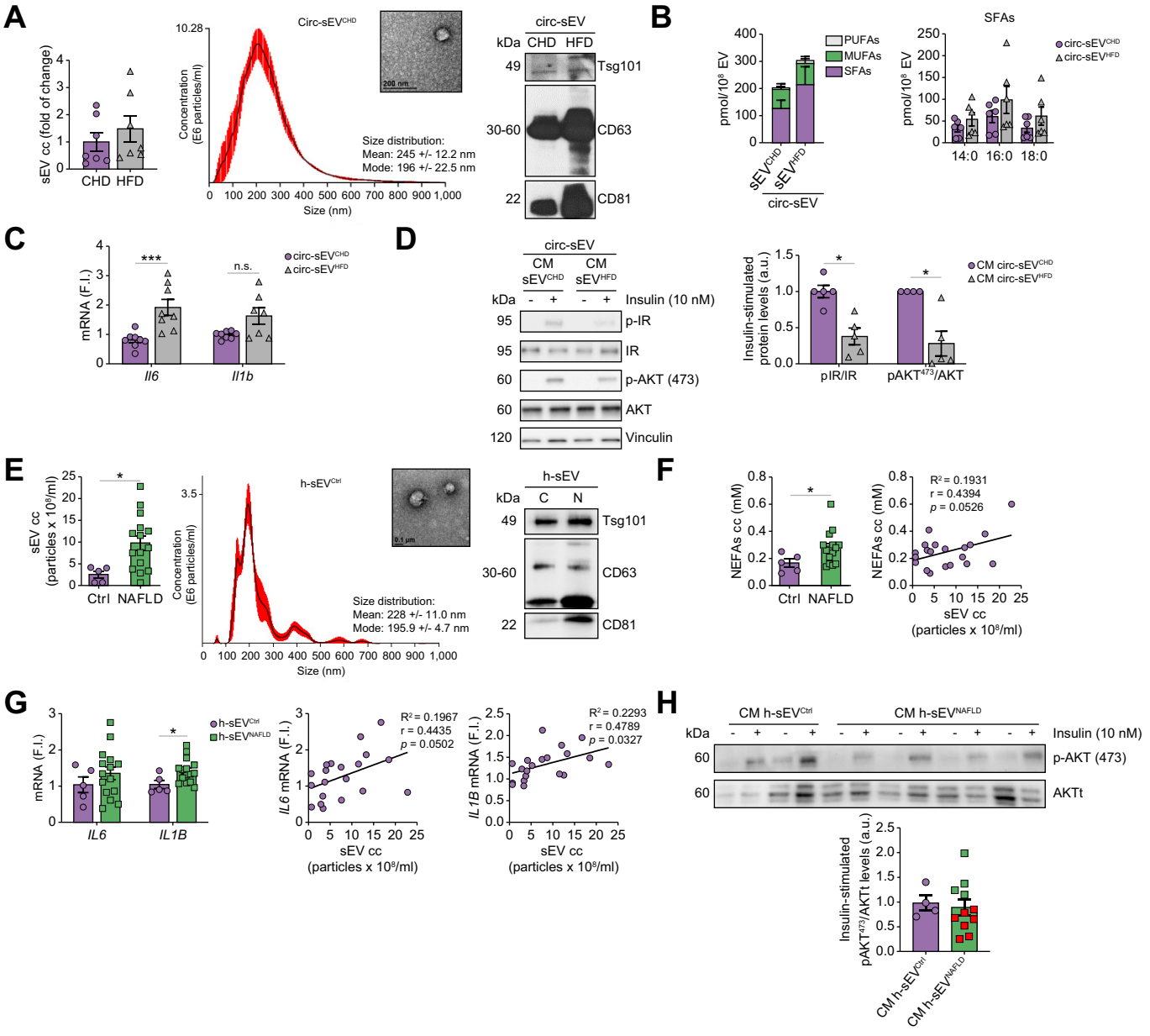

Fig. 8. Circ-sEV from obese mice with NAFLD and patients with NAFLD are elevated in plasma and induce inflammation in macrophages and insulin resistance in hepatocytes. (A) NTA quantification of Circ-sEV (n = 7/group) (left panel). Representative image of NTA and TEM photomicrograph from Circ-sEV^{CHD} (scale bar, 200 nm) (middle panel). Expression of sEV markers and calnexin in Circ-sEV (right panel). (B) Total FFA content (left) and SFA distribution (right) in Circ-sEV are shown (n = 6/group). (C) *Il-6* and *Il-1β* mRNAs in peritoneal macrophages incubated with Circ-EV for 8 h (n = 7–8/group). (D) Peritoneal macrophages were incubated with Circ-sEV^{C} for 24 h and the CM was used to treat PH for 24 h prior to insulin stimulation (10 min, 10 nM). Representative Western blots and quantification (n = 4–5/group). (E) NTA quantification of Circ-sEV in plasma from healthy individuals (Ctrl, n = 5) and patients with NAFLD (NAFLD, n = 15) (left panel). Representative image of NTA and TEM photomicrograph (scale bar, 0.1 μm) from healthy h-sEV^{Ctrl} (middle panel). Expression of sEV markers in h-sEV (right panel). (F) Quantification of circulating NEFAs (left panel) in healthy individuals (Ctrl, n = 5) and patients with NAFLD (NAFLD, n = 15). Correlation between the amount of sEV and NEFAs in plasma (right panel). (G) h-MFs were incubated for 8 h with h-sEV^{Ctrl} or h-sEV^{NAFLD}. *IL-6* and *IL-1β* (beta) mRNAs (left panel). Correlation between the amount of sEV in plasma and *IL-6* and *IL-1β* (beta) mRNAs in h-MFs treated with the sEV (middle and right panels, respectively). (H) h-MFs were incubated for 24 h with sEV from plasma of control individuals or patients with NAFLD. The CM was used to treat HuH7 human hepatocytes for 24 h before insulin stimulation (10 min, 10 nM). Representative Western blots and quantification (Ctlr, n = 4; patients with NAFLD, n = 11). Data are expressed as the mean ± SEM. In (C) and (D), $^{*}p$ <0.05, $^{***}p$ <0.001, compared with Circ-sEV^{CHD}, Mann–Whitney *U* test. In (E–G), $^{*}p$ <0.05, compared with h-sEV^{Ctrl}, Mann–Whitney *U* test. a.u., arbitrary units; cc, concentration; CHD, chow diet; Circ-sEV, circulating sEV; CM, conditioned medium; FI, fold induction; FFA, free fatty acid; h-MF, human macrophage; HFD, high-fat diet; IR, insulin receptor; MUFA, monounsaturated fatty acid; NAFLD, non-alcoholic fatty liver disease; NEFA, non-esterified fatty acid; NTA, nanoparticle tracking analysis; PUFA, polyunsaturated fatty acid; sEV, small extracellular vesicles; SFA, saturated fatty acid; TEM, transmission electron microscopy.

humans with NAFLD in macrophage inflammation and insulin signalling in hepatocytes. Fig. 8A and Fig. S12A show the characterisation of Circ-sEV from mice fed a CHD or HFD (Circ-sEV^{CHD} and Circ-sEV^{HFD}, respectively). A slight increase in sEV number was found in Circ-sEV^{HFD} compared with Circ-sEV^{CHD}. Lipidomic analysis of Circ-sEV revealed increased SFA (non-significant) content in Circ-sEV^{HFD} compared with Circ-sEV^{CHD} (Fig. 8B and Table S5). Importantly, Circ-sEV^{HFD} triggered inflammation in peritoneal macrophages (Fig. 8C), an effect also observed in macrophages loaded with sEV isolated from the plasma of mice fed a MCD diet (Circ-sEV^{MCD}) (Fig. S13). Moreover, insulin resistance was found in PH pretreated with the CM released from peritoneal macrophages loaded with Circ-sEV^{HFD} (Fig. 8D). Of note, IR and AKT phosphorylation in hepatocytes did not change upon stimulation with CM from macrophages treated with Circ-sEV^{CHD} compared with those treated with CM from unstimulated macrophages (Fig. S14).

To add translational relevance to our study, we purified sEV from the serum of a cohort of 15 patients with NAFLD (Table S6) and healthy individuals. After characterisation (Fig. 8E and Fig. S12B), we found increased Circ-sEV in patients with NAFLD (h-sEV^{NAFLD}) compared with healthy controls (h-sEV^{Ctrl}). The amount of Circ-sEV in patients with NAFLD correlated with circulating non-esterified fatty acids (NEFAs) (Fig. 8F) and dyslipidaemia (Table S7). sEV were used to treat human macrophages (h-MFs). *IL-1β* (beta) expression significantly increased in h-MFs receiving circulating h-sEV^{NAFLD}, and a correlation between *IL-1β* (beta) and *IL-6* expression and circulating h-sEV-^{NAFLD} was found (Fig. 8G). *IL-1β* (beta) mRNA also correlated with dyslipidaemia and transaminases in patients with NAFLD (Table S7). Finally, as occurred in mice, CM from h-MFs receiving h-sEV^{NAFLD} decreased insulin-induced AKT phosphorylation in HuH7 human hepatocytes, an effect evidenced in seven patients with NAFLD from a subcohort of 11 individuals (Fig. 8H).

Discussion

Herein, we identified, for the first time, an interactome by which hepatocytes under lipotoxic stress secrete SFA-loaded sEV that target liver macrophages/KC via TLR4-mediated signalling, triggering a pro-inflammatory response, which, in turn, attenuates insulin signalling in hepatocytes.

Several molecules have been identified in the cargo of sEV released by lipotoxic hepatocytes including miRNAs,[26,27] proapoptotic molecules (*e.g.* TRAIL),[16] or chemotaxis mediators (*e.g.* C-X-C motif chemokine ligand 10 [CXCL10]).[28] Regarding bioactive lipid species, the presence of C16:0 ceramide,[29] as well as sphingosine 1-phosphate,[30] has been reported as cargo of EV released by hepatocytes exposed to lipotoxicity. Herein, we show an enrichment in SFAs, particularly PA and SA, in sEV released by lipotoxic hepatocytes either treated with PA or, importantly, directly isolated from obese mice fed a HFD with manifested features of fatty liver. These results suggest hepatocyte-released sEV as new carriers of different toxic lipid species with cell/tissue specificity. In addition, the release of SFA-enriched sEV by hepatocytes under lipotoxic stress might represent an escape route to reduce their lipid overload and, therefore, to avoid hepatocyte toxicity.

In the context of cell-to-cell lipid transmission, lipid transport to recipient cells is mediated not only by canonic carrier proteins and lipoproteins, but also by sEV, as reviewed.[31] It has been calculated that internalisation of sEV into endosomes of target cells allows 500 times higher concentrations of prostaglandins than the concentrations reached if they had been directly added to the whole cell.[32] In this scenario, macrophages are the main target cells of sEV;[33] therefore, they are likely direct recipients of the lipotoxic cargo of the hepatocyte-released EV in NAFLD. In this regard, we have characterised *in vitro* the trafficking of hepatocyte-released sEV to the macrophages, as reported,[16] and provided details of their uptake by the endosomal pathway. Moreover, in the recipient macrophages, lipidomic analysis revealed increased content of PA and SA, highly lipotoxic and pro-inflammatory SFAs contained in sEV. These results suggest the transfer of SFAs from hepatocytes to macrophages via sEV likely resulting in the activation of pro-inflammatory signalling (JNK, P38 MAPK, and p65-NF-κB), the elevation of pro-inflammatory cytokine mRNAs (*Il-6*, *Il-1β*, and *Tnf*), and the upregulation of the chemokine *Ccl2*. Notably, the anti-inflammatory *Il-10* mRNA was also increased by sEV^{PA}, pointing to the activation of survival pathways in macrophages for counteracting inflammation. Furthermore, the lipids extracted from sEV released by lipotoxic hepatocytes were enough to switch macrophages to an M1 profile. These results support the importance of hepatocyte-released sEV as reactive lipid carriers in the interactome with macrophages. In a more physiological context, KC were also targets of lipotoxic hepatocyte-released sEV, an effect manifested by increases in PA/SA content, and *Il-6*, *Il-1β*, and *Tnf* mRNAs, as well as the release of IL-1β to the culture medium. It is also noteworthy to highlight that the requirement of fetuin A as an adaptor protein in lipid-induced TLR4 activation in adipocytes has been reported.[34] Thus, a role for fetuin A in mediating the pro-inflammatory effects of lipotoxic sEV cannot be ruled out.

Despite the controversy on the role of TLR4 as an SFA receptor,[35] it has been extensively reported that SFAs promote the translocation of TLR4 into lipid rafts in the plasma membrane for subsequent TLR4/myeloid differentiation factor 2 (MD2) complex dimerisation and endocytosis in different cell types including macrophages/KC, driving the outcome of pro- or anti-inflammatory responses.[22,36,37] Moreover, TLR4-mediated inflammatory responses have been reported in THP-1 macrophages exposed to sEV derived from different body fluids[38] and, more importantly, in macrophages exposed to adipose-tissue-derived sEV.[39] Herein, we show, on the one hand, a rapid downregulation of TLR4 protein levels, which has been related to its activation as mentioned above,[40] in macrophages receiving hepatocyte-derived lipotoxic sEV and, on the other, a marked effect of TLR4 deficiency or pharmacological inhibition in attenuating M1 pro-inflammatory signalling (*i.e.* IκBα degradation, p65-NF-κB nuclear translocation, and gene expression signature) in peritoneal macrophages/KC. In agreement, other studies have demonstrated that disruption of TLR4 function ameliorates hepatic inflammation, steatosis, and fibrosis in NAFLD rodent models.[41] In addition, TLR4 expression is upregulated in the livers of patients with NASH, compared with those with fatty liver.[42] In this line, our study has identified, for the first time, macrophage TLR4 as a target of hepatocyte-derived sEV in the context of lipotoxicity in NAFLD. Of note, whether direct contact of the sEV with TLR4 at the cell surface or in endosomes trigger sEV pro-inflammatory effects deserves further investigation.

Insulin resistance in hepatocytes is a feature of NAFLD, steatosis and inflammation being negative modulators of insulin action.[43] Initially, we tested a possible direct (autocrine) effect of

lipotoxic sEV in hepatocytes, but we did not find substantial impairment of IR/AKT phosphorylation. Because in a previous study we found attenuated insulin signalling in hepatocytes exposed to the CM from PA-treated macrophages,[21] we wondered whether the CM released by macrophages exposed to PA/SA-enriched sEV containing IL-6 and IL-1β and, likely, other pro-inflammatory mediators could recapitulate this alteration. Remarkably, hepatocytes exposed to CM-sEV^{PA} or CM-sEV^{HFD} showed decreased IR/AKT phosphorylation in response to insulin. In a more physiological context, the CM released by KC loaded with lipotoxic sEV also decreased insulin-induced phospho-AKT in hepatocytes. This hepatocyte–macrophage/KC–hepatocyte paracrine crosstalk within liver cells, likely mediated by SFA-containing sEV, was not reported before. In that regard, selective depletion of KC ameliorated steatosis and insulin resistance in mice.[44]

To provide *in vivo* findings of sEV lipotoxic effects, we injected mice with sEV^{PA} or sEV^{HFD} and found features of hepatic inflammation compared with those in mice injected with sEV^{C}. At the molecular level, a rapid reduction of TLR4 expression that concurred with increased phospho-JNK and pro-inflammatory gene expression shed light on the potent effect of lipotoxic sEV in inducing local liver inflammation. Our results are in line with the liver inflammation reported when sEV released by inositol-requiring enzyme-1α (IRE1α)-overexpressing hepatocytes were injected into mice and reached the liver promoting monocyte infiltration.[45] By contrast, we found a rapid accumulation of PKH26-labelled sEV in liver KC rather than hepatocytes, suggesting that resident macrophages are early targets of the sEV. In fact, KC are the predominant cell type that takes up sEV released by pancreatic cancer cells.[46] Importantly, evaluation of nuclear p65-NF-κB translocation in response to lipotoxic sEV showed a cell-specific biphasic pattern with marked immunostaining at 30 min post injection in immune cells and thereafter in hepatocytes at 2 h, an effect correlating with elevations in pro-inflammatory genes. Likewise, *Ccl2* expression was elevated at 2 h, the time period at which infiltration of monocytes and lymphocytes was observed. Of relevance, p65-NF-κB nuclear translocation in hepatocytes and monocyte/lymphocyte infiltration were absent in mice injected the TLR4 inhibitor before sEV^{PA}, recapitulating the *in vitro* results. Similar protection against liver inflammation induced by lipotoxic sEV was obtained in mice with specific deletion of TLR4 in myeloid cells, reinforcing the role of TLR4 as a mediator of the lipotoxic EVs in liver inflammation. Moreover, haematopoietic cell-specific deletion of TLR4 was able to ameliorate diet-induced insulin resistance in the liver and adipose tissue.[47] In this regard, our data show that the insulin response of the hepatocytes exposed to the CM released by KC from TLR4$^{-/-}$ mice loaded with lipotoxic sEV was higher than that of the hepatocytes treated with the CM released by KC from control mice.

In addition to the local effects in the liver, in a systemic context, Circ-sEV from obese mice activated a pro-inflammatory response in macrophages and produced a CM that decreased IR/AKT phosphorylation in hepatocytes. These results point that, during obesity, both the intrahepatic interactome and the sEV released to the circulation by peripheral tissues (mainly adipose tissue) boost insulin resistance. Of note, systemic insulin resistance was found in lean mice chronically injected Circ-sEV from diet-induced obese mice[48] or adipose tissue-derived exosomes from *ob/ob* mice.[49] Interestingly, an inflammatory response of macrophages was also observed upon treatment with Circ-sEV from lean mice fed an MCD diet in which adipose tissue was almost absent, suggesting a potential pro-inflammatory effect of liver-derived sEV under this pathological condition. However, we cannot rule out the distinct origin of lipotoxic sEV (*e.g.* adipose tissue) in the circulation in patients with NAFLD.

The translational relevance of the macrophage–hepatocyte crosstalk mediated by lipotoxic sEV was evidenced by reduced insulin-mediated AKT phosphorylation in human hepatocytes exposed to the CM from h-MFs loaded with sEV from patients with NAFLD. In addition, the more abundance of Circ-sEV in patients with NAFLD, which correlated with NEFA levels, together with their inflammatory effect on naïve macrophages, points to these lipotoxic species as possible cargo of the sEV and, therefore, as mediators of the hepatocyte–macrophage interactome in human NAFLD.

In conclusion, we have identified SFAs as essential components of the cargo in sEV released by the hepatocytes under NAFLD conditions that are transferred to macrophages/KC and, via TLR4, trigger liver inflammation and insulin resistance in hepatocytes. Evidence of this macrophage–hepatocyte interactome was also found in patients with NAFLD, pointing to the relevance of sEV as additional SFA transporters and mediators of lipotoxicity in NAFLD. Therapeutic interventions targeting TLR4-mediated pro-inflammatory signalling in this crosstalk would open new opportunities in the early prevention of NAFLD. This study also opens a new perspective regarding the role of SFA bioactive lipid cargo in sEV. In this context, owing to sEV availability in biological fluids, lipotoxic lipids contained in sEV are proposed to be promising non-invasive biomarkers in liquid biopsy,[25,39] which indeed would help in improving NAFLD diagnosis. More research will establish whether lipotoxic SFAs into sEV may be potential therapeutic targets for NAFLD treatment.

Abbreviations

a.u., arbitrary units; cc, concentration; CHD, chow diet; Circ-sEV, circulating sEV; CM, conditioned medium; CXCL10, C-X-C motif chemokine ligand 10; EEA1, early endosome antigen 1; EV, extracellular vesicles; FFA, free fatty acid; FI, fold induction; h-MF, human macrophage; HFD, high-fat diet; HPF, high-power field; IR, insulin receptor; IRE1α, inositol-requiring enzyme-1α; JNK, Jun N-terminal kinase; KC, Kupffer cells; MCD, methionine–choline deficient; MISEV, Minimal Information for Studies of Extracellular Vesicles; MUFA, monounsaturated fatty acid; NAFLD, non-alcoholic fatty liver disease; NASH, non-alcoholic steatohepatitis; NEFA, non-esterified fatty acid; NTA, nanoparticle tracking analysis; PA, palmitic acid; PH, primary hepatocytes; PUFA, polyunsaturated fatty acid; rM, recipient macrophages; sEV, small extracellular vesicles; SFA, saturated fatty acid; SA, stearic acid; sPH, secreting PH; TEM, transmission electron microscopy; TLR4, Toll-like receptor-4; TLR4i, TLR4 inhibitor; TRAIL, tumour necrosis factor-related apoptosis-inducing ligand.

Financial support

This work was supported by grants PID2021-122766OB-I00 (AMV), PID2019-105989RB-I00 (JB), PID2020-113238RB-I00 (LB), PID2019-106581RB-I00 (MAM), PID2020-114148RB-I00 (MI), PID2019-107036RB-I00 (RF), and RD21/0006/0001 (ISCIII) (IL) funded by Ministerio de Ciencia e Innovación/Agencia Estatal de Investigación/10.13039/501100011033 and ERDF 'A way of making Europe' by the European Union

(MICINN/AEI/FEDER, EU), grant EFSD/Boehringer Ingelheim European Research Programme on 'Multi-System Challenges in Diabetes' from the European Foundation for the Study of Diabetes (AMV), P2022/BMD-7227 (Comunidad de Madrid, Spain) (AMV), Fundación Ramón Areces (Spain) (AMV), CIBERdem (AMV and JB), CIBERhed (RF), and CIBERcv (LB) (ISCIII, Spain). LB and AMV belong to the Spanish National Research Council's (CSIC's) Cancer Hub. We also acknowledge the Spanish Ministry of Economy and Competitiveness (MINECO) postdoctoral contract IJCI-2015-24758 to IGM and the Spanish Ministry of Education, Culture and Sport (MECD) FPU17/02786 grant to RA.

Conflicts of interest

The authors declare no conflicts of interest related to this work.

Please refer to the accompanying ICMJE disclosure forms for further details.

Authors' contributions

Conducted study design: IGM, RA, AMV. Conducted data acquisition and analysis: IGM, RA. Conducted manuscript drafting and revision: IGM, RA, AMV. Conducted lipidomic analysis: LP, AA. Conducted Western blots: ABH. Contributed human samples: IGH, RF. Conducted human macrophage isolation: APR. Contributed human macrophages: ELC, LB. Contributed to manuscript revision: LB, RF, IL, MAM, JB, MI. Contributed mouse models: IL, MAM. Conducted the analysis and interpretation of lipidomic data: JB. Contributed to data analysis of sEV by NTA: MI. Coordinated the study: AMV.

Data availability statement

The data that support the findings of this study are available from the corresponding authors upon reasonable request.

Acknowledgements

We acknowledge Mónica M. Belinchón and Lucía Guerrero (IIBm, CSIC, Madrid, Spain) for technical assistance with confocal microscopy. We also acknowledge N. Nieto and lab members (University of Chicago, USA) for helpful discussions.

Supplementary data

Supplementary data to this article can be found online at https://doi.org/10.1016/j.jhepr.2023.100756.

References

Author names in bold designate shared co-first authorship.

[1] Younossi ZM, Koenig AB, Abdelatif D, Fazel Y, Henry L, Wymer M. Global epidemiology of nonalcoholic fatty liver disease-Meta-analytic assessment of prevalence, incidence, and outcomes. Hepatology 2016;64:73–84.
[2] Banini BA, Sanyal AJ. Nonalcoholic Fatty liver disease: epidemiology, pathogenesis, natural history, diagnosis, and current treatment options. Clin Med Insights Ther 2016;8:75–84.
[3] **Eslam M**, **Newsome PN**, Sarin SK, Anstee QM, Targher G, Romero-Gomez M, et al. A new definition for metabolic dysfunction-associated fatty liver disease: an international expert consensus statement. J Hepatol 2020;73:202–209.
[4] Adams LA, Ratziu V. Non-alcoholic fatty liver – perhaps not so benign. J Hepatol 2015;62:1002–1004.
[5] Béland-Bonenfant S, Rouland A, Petit JM, Vergès B. Concise review of lipidomics in nonalcoholic fatty liver disease. Diabetes Metab 2023;49:101432.
[6] Musso G, Cassader M, Paschetta E, Gambino R. Bioactive lipid species and metabolic pathways in progression and resolution of nonalcoholic steatohepatitis. Gastroenterology 2018;155:282–302.e8.
[7] Shen C, Ma W, Ding L, Li S, Dou X, Song Z. The TLR4-IRE1α pathway activation contributes to palmitate-elicited lipotoxicity in hepatocytes. J Cel Mol Med 2018;22:3572–3581.
[8] Rivera CA, Adegboyega P, van Rooijen N, Tagalicud A, Allman M, Wallace M. Toll-like receptor-4 signaling and Kupffer cells play pivotal roles in the pathogenesis of non-alcoholic steatohepatitis. J Hepatol 2007;47:571–579.
[9] Kazankov K, Jørgensen SMD, Thomsen KL, Møller HJ, Vilstrup H, George J, et al. The role of macrophages in nonalcoholic fatty liver disease and nonalcoholic steatohepatitis. Nat Rev Gastroenterol Hepatol 2019;16:145–159.
[10] Arrese M, Cabrera D, Kalergis AM, Feldstein AE. Innate immunity and inflammation in NAFLD/NASH. Dig Dis Sci 2016;61:1294–1303.
[11] **Malloci M**, **Perdomo L**, Veerasamy M, Andriantsitohaina R, Simard G, Martínez MC. Extracellular vesicles: mechanisms in human health and disease. Antioxid Redox Signal 2019;30:813–856.
[12] Kalluri R, LeBleu VS. The biology, function, and biomedical applications of exosomes. Science 2020;367:eaau6977.
[13] Théry C, Witwer KW, Aikawa E, Alcaraz MJ, Anderson JD, Andriantsitohaina R, et al. Minimal information for studies of extracellular vesicles 2018 (MISEV2018): a position statement of the International Society for Extracellular Vesicles and update of the MISEV2014 guidelines. J Extracell Vesicles 2018;7:1535750.
[14] Xiao Y, Zheng L, Zou X, Wang J, Zhong J, Zhong T. Extracellular vesicles in type 2 diabetes mellitus: key roles in pathogenesis, complications, and therapy. J Extracell Vesicles 2019;8(1):1625677.
[15] Castano C, Novials A, Párrizas M. Exosomes and diabetes. Diabetes Metab Res Rev 2019;35:e3107.
[16] Hirsova P, Ibrahim SH, Krishnan A, Verma VK, Bronk SF, Werneburg NW, et al. Lipid-induced signaling causes release of inflammatory extracellular vesicles from hepatocytes. Gastroenterology 2016;150:956–967.
[17] Mu FT, Callaghan JM, Steele-Mortimer O, Stenmark H, Parton RG, Campbell PL, et al. EEA1, an early endosome-associated protein. EEA1 is a conserved alpha-helical peripheral membrane protein flanked by cysteine "fingers" and contains a calmodulin-binding IQ motif. J Biol Chem 1995;270:13503–13511.
[18] Vitelli R, Santillo M, Lattero D, Chiariello M, Bifulco M, Bruni CB, et al. Role of the small GTPase Rab7 in the late endocytic pathway. J Biol Chem 1997;272:4391–4397.
[19] Tornatore L, Thotakura AK, Bennett J, Moretti M, Franzoso G. The nuclear factor kappa B signaling pathway: integrating metabolism with inflammation. Trends Cel Biol 2012;22:557–566.
[20] Cicuéndez B, Ruiz-Garrido I, Mora A, Sabio G. Stress kinases in the development of liver steatosis and hepatocellular carcinoma. Mol Metab 2021;50:101190.
[21] Pardo V, González-Rodríguez A, Guijas C, Balsinde J, Valverde AM. Opposite cross-talk by oleate and palmitate on insulin signaling in hepatocytes through macrophage activation. J Biol Chem 2015;290:11663–11677.
[22] Shi H, Kokoeva MV, Inouye K, Tzameli I, Yin H, Flier JS. TLR4 links innate immunity and fatty acid-induced insulin resistance. J Clin Invest 2006;116:3015–3025.
[23] Ciesielska A, Matyjek M, Kwiatkowska K. TLR4 and CD14 trafficking and its influence on LPS-induced pro-inflammatory signaling. Cell Mol Life Sci 2021;78:1233–1261.
[24] Weatherill AR, Lee JY, Zhao L, Lemay DG, Youn HS, Hwang DH. Saturated and polyunsaturated fatty acids reciprocally modulate dendritic cell functions mediated through TLR4. J Immunol 2005;174:5390–5397.
[25] **Garcia-Martinez I**, Alen R, Rada P, Valverde AM. Insights into extracellular vesicles as biomarker of NAFLD pathogenesis. Front Med 2020;7:395.
[26] Povero D, Panera N, Eguchi A, Johnson CD, Papouchado BG, de Araujo Horcel L, et al. Lipid-induced hepatocyte-derived extracellular vesicles regulate hepatic stellate cell via microRNAs targeting PPAR-γ. Cell Mol Gastroenterol Hepatol 2015;1:646–663.e4.
[27] **Liu XL**, **Pan Q**, Cao HX, Xin FZ, Zhao ZH, Yang RX, et al. Lipotoxic hepatocyte-derived exosomal microRNA 192-5p activates macrophages through rictor/Akt/forkhead box transcription factor O1 signaling in nonalcoholic fatty liver disease. Hepatology 2020;72:454–469.
[28] Ibrahim SH, Hirsova P, Gores GJ. Non-alcoholic steatohepatitis pathogenesis: sublethal hepatocyte injury as a driver of liver inflammation. Gut 2018;67:963–972.
[29] Kakazu E, Mauer AS, Yin M, Malhi H. Hepatocytes release ceramide-enriched pro-inflammatory extracellular vesicles in an IRE1α-dependent manner. J Lipid Res 2016;57(2):233–245.
[30] Liao CY, Song MJ, Gao Y, Mauer AS, Revzin A, Malhi H. Hepatocyte-derived lipotoxic extracellular vesicle sphingosine 1-phosphate induces macrophage chemotaxis. Front Immunol 2018;9:2980.
[31] Record M, Carayon K, Poirot M, Silvente-Poirot S. Exosomes as new vesicular lipid transporters involved in cell–cell communication and various pathophysiologies. Biochim Biophys Acta 2014;1841:108–120.
[32] Subra C, Grand D, Laulagnier K, Stella A, Lambeau G, Paillasse M, et al. Exosomes account for vesicle-mediated transcellular transport of activatable phospholipases and prostaglandins. J Lipid Res 2010;51:2105–2120.

[33] **Shen M**, **Shen Y**, Fan X, Men R, Ye T, Yang L. Roles of macrophages and exosomes in liver diseases. Front Med 2020;7:583691.
[34] **Pal D**, **Dasgupta S**, Kundu R, Maitra S, Das G, Mukhopadhyay S, et al. Fetuin-A acts as an endogenous ligand of TLR4 to promote lipid-induced insulin resistance. Nat Med 2012;18:1279–1285.
[35] **Lancaster GI**, **Langley KG**, Berglund NA, Kammoun HL, Reibe S, Estevez E, et al. Evidence that TLR4 is not a receptor for saturated fatty acids but mediates lipid-induced inflammation by reprogramming macrophage metabolism. Cell Metab 2018;27:1096–1110.e5.
[36] Lee JY, Ye J, Gao Z, Youn HS, Lee WH, Zhao L, et al. Reciprocal modulation of Toll-like receptor-4 signaling pathways involving MyD88 and phosphatidylinositol 3-kinase/AKT by saturated and polyunsaturated fatty acids. J Biol Chem 2003;278:37041–37051.
[37] Li B, Leung JCK, Chan LYY, Yiu WH, Tang SCW. A global perspective on the crosstalk between saturated fatty acids and Toll-like receptor 4 in the etiology of inflammation and insulin resistance. Prog Lipid Res 2020;77:101020.
[38] **Bretz NP**, **Ridinger J**, Rupp AK, Rimbach K, Keller S, Rupp C, et al. Body fluid exosomes promote secretion of inflammatory cytokines in monocytic cells via Toll-like receptor signaling. J Biol Chem 2013;288:36691–36702.
[39] Srinivas AN, Suresh D, Santhekadur PK, Suvarna D, Kumar DP. Extracellular vesicles as inflammatory drivers in NAFLD. Front Immunol 2020;11:627424.
[40] **Benabid R**, **Wartelle J**, Malleret L, Guyot N, Gangloff S, Lebargy F, et al. Neutrophil elastase modulates cytokine expression: contribution to host defense against *Pseudomonas aeruginosa*-induced pneumonia. J Biol Chem 2012;287:34883–34894.
[41] Ye D, Li FY, Lam KS, Li H, Jia W, Wang Y, et al. Toll-like receptor-4 mediates obesity-induced non-alcoholic steatohepatitis through activation of X-box binding protein-1 in mice. Gut 2012;61:1058–1067.
[42] Sharifnia T, Antoun J, Verriere TG, Suarez G, Wattacheril J, Wilson KT, et al. Hepatic TLR4 signaling in obese NAFLD. Am J Physiol Gastrointest Liver Physiol 2015;309:G270–G278.
[43] Tilg H, Moschen AR, Roden M. NAFLD and diabetes mellitus. Nat Rev Gastroenterol Hepatol 2017;14:32–42.
[44] Huang W, Metlakunta A, Dedousis N, Zhang P, Sipula I, Dube JJ, et al. Depletion of liver Kupffer cells prevents the development of diet-induced hepatic steatosis and insulin resistance. Diabetes 2010;59:347–357.
[45] Dasgupta D, Nakao Y, Mauer AS, Thompson JM, Sehrawat TS, Liao CY, et al. IRE1A stimulates hepatocyte-derived extracellular vesicles that promote inflammation in mice with steatohepatitis. Gastroenterology 2020;159:1487–1503.e17.
[46] Costa-Silva B, Aiello NM, Ocean AJ, Singh S, Zhang H, Thakur BK, et al. Pancreatic cancer exosomes initiate pre-metastatic niche formation in the liver. Nat Cel Biol 2015;17:816–826.
[47] **Saberi M**, **Woods NB**, de Luca C, Schenk S, Lu JC, Bandyopadhyay G, et al. Hematopoietic cell-specific deletion of Toll-like receptor 4 ameliorates hepatic and adipose tissue insulin resistance in high-fat-fed mice. Cel Metab 2009;10:419–429.
[48] Castano C, Kalko S, Novials A, Parrizas M. Obesity-associated exosomal miRNAs modulate glucose and lipid metabolism in mice. Proc Natl Acad Sci U S A 2018;115:12158–12163.
[49] Deng ZB, Poliakov A, Hardy RW, Clements R, Liu C, Liu Y, et al. Adipose tissue exosome-like vesicles mediate activation of macrophage-induced insulin resistance. Diabetes 2009;58:2498–2505.